

FLATBAND POTENTIAL OF TiO₂ SEMICONDUCTOR ELECTRODE

酸化チタン半導体電極のフラットバンドポテンシャル

by FUJISHIMA, Akira, SAKAMOTO, Akira and HONDA Kenichi

藤 嶋 昭*・坂 本 章*・本 多 健 一*

The authors have studied on the photosensitive electrode reaction at semiconductor electrodes. An interesting phenomenon has been found with *n*-type TiO₂ single crystal electrode, which was termed as photosensitized electrolytic oxidation¹⁾. This phenomenon is concerned with the fact that electrolytic oxidation is accelerated owing to light energy absorbed by the semiconductor electrode. Under irradiation of light, oxygen evolution reaction occurred on the semiconductor electrode surface at potentials more positive than about -0.5 V (*vs.* SCE) in a neutral electrolyte solution. This break potential is related to the bending of the energy band near the semi-conductor surface; it corresponds to the so-called flatband potential. It leads to the consideration of the mechanism of photosensitized electrolytic oxidation. The flatband potential is a particularly important factor with semiconductor electrodes²⁾, and almost perfectly analogous to the potential of the electrocapillary maximum at metal electrodes. This paper is concerned with the flatband potential of TiO₂ electrode, which is determined with the charge and potential distribution at the TiO₂-electrolyte interface by measuring the differential capacitance of the semiconductor electrode as a function of applied potential.

Experimental

For semiconductor electrode, *n*-type TiO₂ (rutile type) single crystal wafer was used with (001) face after treating at 700°C (electrode No. 1) and 800°C (electrode No. 2) in 10⁻⁴~10⁻⁵ mmHg atmosphere for about four hours. This wafer was 1.5 mm thick and its surface area was 0.7 cm². Before the experiment the electrode was immersed in the nitric acid aqueous solution for a constant period and then washed with water, so that reproducible data were obtained. The electrolyte solution was the buffered 0.5 normal solution of KCl. The circuit is shown in Fig. 1, which is analogous to that for ZnO electrode reported by Dewald³⁾.

Measurement was made at the frequency of 1 Kc. It was assumed that the interface was represented with an equivalent circuit of *R* and *C* in series and only the capacitance was used here for the purpose of the determination of flatband potentials.

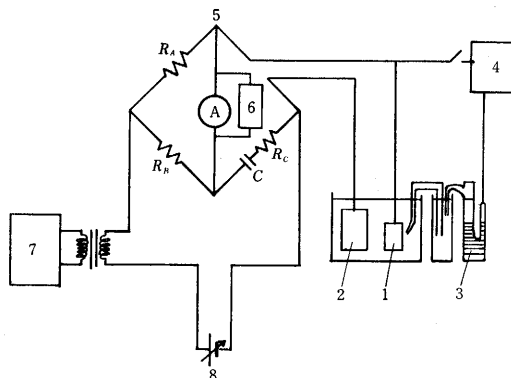


Fig. 1 Apparatus

- | | |
|------------------------------|-----------------------|
| 1 TiO ₂ Electrode | 5 Universal Bridge |
| 2 Pt Counter Electrode | 6 Tuned Null Detector |
| 3 S. C. E. | 7 Oscillator |
| 4 Voltmeter | 8 Dry Cell |

Results and Discussion

The space charge layer of an *n*-type semiconductor electrode at the interface between electrode and electrolyte changes from exhaustion layer to flatband condition, and further to accumulation layer⁴⁾, as the electrode is polarized from anodic region to cathodic. The capacitance of the exhaustion layer is generally much smaller than that of the Helmholtz layer, hence the capacitance of these regions in series is effectively the capacitance of the exhaustion layer alone and the applied potential drops almost entirely in this region. The theory relating to capacitance per unit area, *C_s*, and potential, *V*, across an exhaustion layer shows the following relation,

$$\frac{d(1/C_s)}{dV} = \frac{2}{q\epsilon\epsilon_0 N_D} \quad (1)$$

where *q* is the electronic charge, ϵ the relative dielectric constant, and *N_D* the donor density. In

* 東京大学生産技術研究所 第4部

general when the $1/C_s^2 \sim V$ curve is extrapolated, the interception of V axis gives the flatband potential.

The capacitance of the TiO_2 electrode was larger than that of ZnO , since TiO_2 is one of the strong dielectric substances, its dielectric constant being 173⁶⁾. Fig. 2 shows the plots of the reciprocal of the squared value of capacitance against the electrode potential for electrodes 1 and 2. As can be seen, in the highly anodic polarization region the resulting curves are linear but in the region of weakly anodic polarization these curves shift greatly from linear lines. This fact may be due to the assumption that the capacitance of the Helmholtz layer, C_H , is larger than that of the space charge layer, C_s , so that C_H has little contribution to total capacitance. Therefore, the values of C_s were calculated by substituting various values for C_H in the equation (2) as a parameter.

$$\frac{1}{C} = \frac{1}{C_H} + \frac{1}{C_s} \quad (2)$$

Fig. 3 and Fig. 4 show the relation between $1/C_s^2$ and V for electrode 1 and electrode 2, respectively. When C_H was $3.0 \mu F$ for electrode 1 and $6.2 \mu F$ for electrode 2, linear lines were obtained. From the interception of V axis, both electrodes gave the same value $-0.50 V$, which correspond to the flatband potential of the TiO_2

electrode in the pH 4.7 electrolyte solution. This value also agrees with the break potential of the current-voltage curve of the same pH electrolyte solution under irradiation. This fact indicates that the mechanism of the photosensitized electrolytic oxidation due to band structure is reasonable.

When current-voltage curves were measured potentiostatically in solutions of various pH values, the break potentials shifted towards more cathodic as the pH of the buffered electrolyte solution was higher. The relationship of the flatband potential

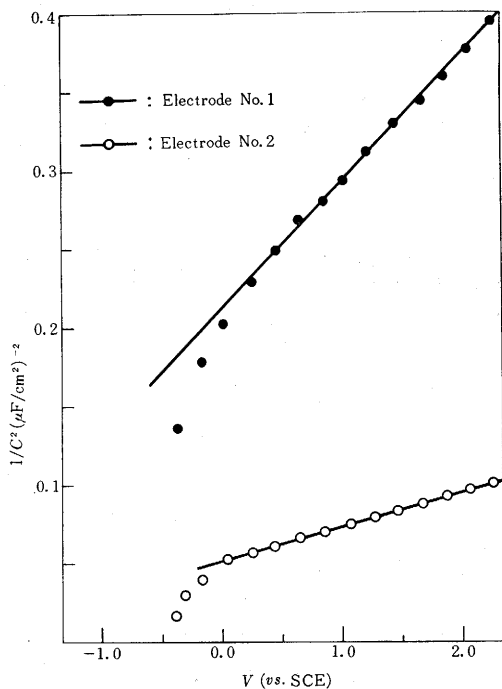


Fig. 2 Relation between V and $1/C^2$

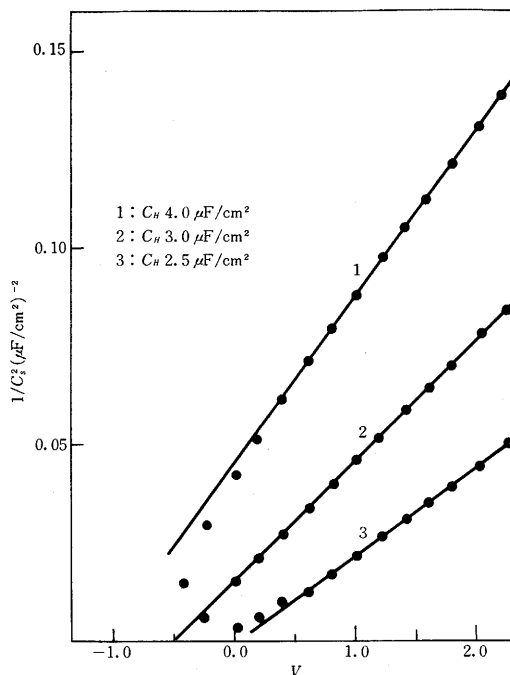


Fig. 3 Relation between $1/C_s^2$ and V for Electrode 1

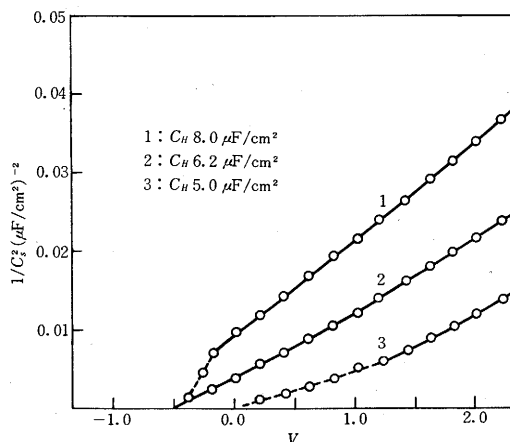


Fig. 4 Relation between $1/C_s^2$ and V for Electrode 2

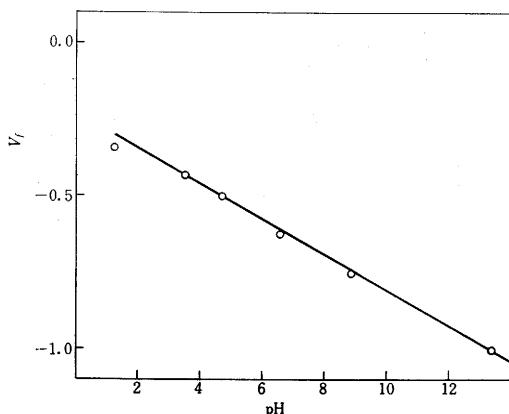
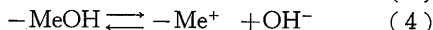
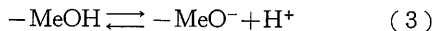


Fig. 5 Relation between flatband potential and pH

to pH is shown in Fig. 5, where a linear line with the slope of about 59 mV/pH was obtained.

Dependence of an electrical double layer on pH at a metal oxide-solution interface is the result of the adsorbed hydrogen or hydroxyl ions, or dissolution occurring at the surface⁷⁾. This may be considered as follows; equilibrium at the oxide-electrolyte interface is established in the following way;



If the potential of the electrolyte solution is zero as reference potential, from the equation (3) and (4) the equilibrium condition is obtained,

$$\begin{aligned} \mu_{\text{MeOH}}^{\circ} + RT \ln a_{\text{MeOH}} \\ = \mu_{\text{MeO}^-}^{\circ} + RT \ln a_{\text{MeO}^-} + \mu_{\text{MeO}^-}^{\circ*} \\ + RT \ln a_{\text{MeO}^-*} + \mu_{\text{H}^+}^{\circ} + RT \ln a_{\text{H}^+} - F\varphi \end{aligned} \quad (5)$$

$$\mu_{\text{MeOH}}^{\circ} + RT \ln a_{\text{MeOH}}$$

$$\begin{aligned} = \mu_{\text{Me}^+}^{\circ} + RT \ln a_{\text{Me}^+} + \mu_{\text{Me}^+}^{\circ*} \\ + RT \ln a_{\text{Me}^+*} + \mu_{\text{OH}^-}^{\circ} + RT \ln a_{\text{OH}^-} + F\varphi \end{aligned} \quad (6)$$

where MeO^- and Me^+ represent the species of the dissolved ions and MeO^-* and Me^+* the adsorbed species. From (5) and (6), equation (7) and (8) are obtained, respectively,

$$\varphi = K_1 + \frac{RT}{F} \ln \frac{a_{\text{MeO}^-} \cdot a_{\text{MeO}^-*}}{a_{\text{MeOH}}} - \frac{2.3 RT}{F} \text{pH} \quad (7)$$

$$\varphi = K_2 + \frac{RT}{F} \ln \frac{a_{\text{MeOH}}}{a_{\text{Me}^+} \cdot a_{\text{Me}^+*}} - \frac{2.3 RT}{F} \text{pH} \quad (8)$$

From (7) and (8) the next equation is obtained,

$$\varphi = K_3 + \frac{RT}{2F} \ln \frac{a_{\text{MeO}^-} \cdot a_{\text{MeO}^-*}}{a_{\text{Me}^+} \cdot a_{\text{Me}^+*}} - \frac{2.3 RT}{F} \text{pH}$$

TiO_2 is chemically stable, but if it dissolves a little, the second term of the equation (9) will very greatly participate in φ . However, the experimental result showed $\frac{d\varphi}{d\text{pH}}$ of about 59 mV/pH, indicating that TiO_2 does not dissolve at all.

References

- 1) A. Fujishima, K. Honda and S. Kikuchi, *J. Chem. Soc. Japan, Industrial Chemistry Section (Kogyo Kagaku Zasshi)*, **72**, 108 (1969).
- 2) W. H. Bratten and C. G. B. Garrett, *Bell System Tech. J.*, **34**, 129 (1955).
- 3) J. F. Dewald, *Bell System Tech. J.*, **37**, 615 (1960).
- 4) H. U. Harten, *Electrochim. Acta*, **13**, 1255 (1968).
- 5) P. J. Boddy, *J. Electrochem. Soc.*, **115**, 199 (1968).
- 6) F. A. Grant, *Rev. Modern phys.*, **31**, 646 (1959).
- 7) G. A. Parks, *Chem. Rev.*, **65**, 177 (1965).

p. 39 よりつづく

でラジカルが生成すると考えられるが、分解温度 650°C 近辺ではスチレンの方が β -メチルスチレンよりはるかに熱安定性が大きく、したがって生成物の安定性から考えて、反応は(1)の位置にラジカルを生成する経路、すなわちスチレンが生成する経路が優先するものと考えられる。

4. 総括

AS 共重合体と AMS 共重合体の熱分解機構は全く同じであるとはいえないが、比較検討により、次のことが明らかになった。

1) AS 共重合体の熱分解ではアセトニトリルに境界効果が見られた。

2) 低温と高温でアセトニトリルの生成経路が異なる。

3) AMS 共重合体の熱分解では、構成モノマーの生成経路が低温と高温で異なる。

4) 以上のことから、AS 共重合体の熱分解においても、構成モノマーであるスチレンの生成経路は一通りではなく、温度により異なることが推測された。

(1969年4月25日受理)

文献

- 1) A. Barlow, et al., *Polymer*, **2**, 27 (1961)
- 2) K. J. Bombaugh, et al., *Anal. Chem.*, **35**, 1834 (1963)
- 3) J. van Schooten, et al., *Polymer*, **6**, 343 (1965)
- 4) Y. Shibasaki, *J. Polymer Sci., A-1*, **5**, 21 (1967)
- 5) G. Nencini, *Polymer Letters*, **3**, 483 (1965)